PHYSICAL REVIEW A VOLUME 23, NUMBER 3 MARCH 1981

Diagrammatic representation of photon echoes and other laser-induced ordering processes in gases

T. W. Mossberg and S. R. Hartmann
Columbia Radiation Laboratory, Department of Physics, Columbia University, New York, New York 10027
(Received 7 October 1980)

A simple diagrammatic approach to the description of laser-induced macroscopic ordering processes in gases is developed. We derive a set of simple rules which can be used to construct diagrams—each of which represents the macroscopic properties of a gaseous sample after it has been excited by a particular sequence of short, resonant, laser-excitation pulses. The features of the diagrams which signify various forms of laser-induced macroscopic ordering, e.g., photon echoes, grating echoes, stimulated echoes, standing-wave echoes, trilevel echoes, nonthermal velocity distributions, etc., are discussed. Important differences between the actions of traveling-wave and standing-wave excitation pulses are pointed out. The diagrammatic technique presented here for gases can easily be generalized to describe laser-induced macroscopic ordering in solids as well.

I. INTRODUCTION

The dynamics of laser-induced reordering processes (such as those involved in optical echo formation[1-20]) possess an essential simplicity which is often obscured in standard density-matrix-type analyses.[21-27] In certain cases (e.g., that of the two-pulse photon echo), a vector-model analysis[28,29] of the effect of a laser-excitation-pulse sequence provides an excellent picture of the reordering dynamics. Unfortunately, however, the vector model is limited to the description of reordering processes which occur in samples of what are basically two-level atomic systems. In this paper, we present a simple diagrammatic approach to the description of reordering processes (of which optical echoes are a subset) which is both widely applicable and intuitively satisfying. Simple rules allow the construction of diagrams which map out in time the coherences in *phase* or *population* which are generated in a sample by any sequence of laser-excitation pulses. We will concentrate here on the analysis of laser-induced ordering in gases, but the diagrammatic approach developed here is easily applied to solids as well.

II. PARTIAL STATE AMPLITUDES

A. Definitions

We deal with an optically thin gaseous sample of atoms which are identical except with regards to their velocity and position. In the absence of external fields each atom is described by a Hamiltonian H_0. The atoms have eigenstates $|s\rangle$ which satisfy

$$H_0|s\rangle=\hbar\Omega_s|s\rangle . \tag{1}$$

For convenience, we assume that the eigenstates are nondegenerate and we neglect relaxation processes. The sample is to be irradiated by a series of laser-excitation pulses which cause immediate and delayed ordering. In general, we can write an atom's wave function as

$$\psi(t)=\sum_s A^s \exp(-i\Omega_s t)|s\rangle , \tag{2}$$

where the state amplitudes A^s are constants except when being modified by the laser-excitation pulses. As will become clear below, it is useful to decompose the state amplitudes A^s into a series of *partial state amplitudes* (PSA's) each of which is labeled according to its historical development. We write

$$A^s=\sum_i a_i^s , \tag{3}$$

where the superscripts denote the eigenstate with which the PSA is associated and the subscripts differentiate between PSA's with distinct histories. We sometimes find it useful to explicitly indicate the number of times that laser pulses have caused a change in the amplitude of a particular PSA (or its precursor) without changing its index s. To show that n_r such changes have taken place in the historical development of the PSA a_i^s we write $a_i^s(n_r)$.

B. Response of an atom to laser excitation in terms of its PSA's

Consider a single atom initially residing solely in a particular state $|l\rangle$ [see Fig. 1(a)]. The atom's initial wave function consists of a single term and is given by

$$\psi(t)=a_1^l(0)\exp(-i\Omega_l t)|l\rangle . \tag{4}$$

Let a laser pulse, which is resonant with the transition from the state $|l\rangle$ to another state $|m\rangle$

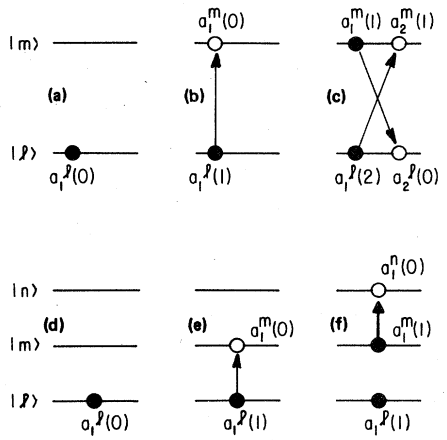

FIG. 1. The *partial state amplitudes* (PSA's) created in the course of two different excitation schemes. (a)–(c) A single initial PSA, $a_1^l(0)$, is divided, through the action of two successive equal frequency excitation pulses, into a total of four PSA's. (d)–(f) In a three energy-level system, a single PSA is divided by two different frequency excitation pulses into three PSA's.

act on the atom. This laser pulse has the effect of reducing the amplitude of $a_1^l(0)$ and of generating a new PSA $a_1^m(0)$ which is associated with the state $|m\rangle$ [see Fig. 1(b)]. We represent this fact symbolically by writing

$$a_1^l(0) \rightarrow a_1^l(1), a_1^m(0)\,. \tag{5}$$

The PSA $a_1^m(0)$ is said to have been "transferred" to state $|m\rangle$, and the PSA $a_1^l(1)$ "reduced" from $a_1^l(0)$. It follows that after the single-laser excitation pulse, the initial atomic wave function [Eq. (4)] is transformed into

$$\psi(t) = a_1^l(1)\exp(-i\Omega_l t)|l\rangle + a_1^m(0)\exp(-i\Omega_m t)|m\rangle\,. \tag{6}$$

The effect of a second-excitation pulse which is also resonant with the $|l\rangle - |m\rangle$ transition is illustrated in Fig. 1(c) and summarized by the transformation equations

$$a_1^l(1) \rightarrow a_1^l(2), a_2^m(1)\,, \tag{7a}$$

$$a_1^m(0) \rightarrow a_1^m(1), a_2^l(0)\,. \tag{7b}$$

The atomic wave function of Eq. (6) is transformed by the second pulse into

$$\psi(t) = [a_1^l(2) + a_2^l(0)]\exp(-i\Omega_l t)|l\rangle + [a_1^m(1) + a_2^m(1)]\exp(-i\Omega_m t)|m\rangle\,. \tag{8}$$

Generally speaking, an arbitrary PSA, $a_i^s(n_r)$ is transformed by a laser pulse, resonant with the $|s\rangle$-$|s'\rangle$ transition, according to

$$a_i^s(n_r) \rightarrow a_i^s(n_r+1), a_{i'}^{s'}(n_r)\,, \tag{9}$$

where the index i' is chosen to be different from any other subscript already assigned to a PSA associated with the state $|s'\rangle$.

If now a third-excitation pulse is applied (again resonant with the $|l\rangle$-$|m\rangle$ transition), its effect would be

$$\begin{aligned} &a_1^l(2) \rightarrow a_1^l(3), a_3^m(2)\,,\\ &a_2^l(0) \rightarrow a_2^l(1), a_4^m(0)\,,\\ &a_1^m(1) \rightarrow a_1^m(2), a_3^l(1)\,,\\ &a_2^m(1) \rightarrow a_2^m(2), a_4^l(1)\,, \end{aligned} \tag{10}$$

and so on.

Not all laser-excitation pulses need be resonant with the same transition. Suppose a total of two pulses are applied, the first resonant with the $|l\rangle$-$|m\rangle$ transition and the second resonant with the $|m\rangle$-$|n\rangle$ transition, where $|n\rangle$ represents another distinct energy state. The effect would be as illustrated in Figs. 1(d)–(f). Assume as before that the atom is initially in the state $|l\rangle$ and that the only nonzero PSA is $a_1^l(0)$. The first pulse then causes

$$a_1^l(0) \rightarrow a_1^l(1), a_1^m(0)\,, \tag{11a}$$

while the second pulse causes

$$a_1^m(0) \rightarrow a_1^m(1), a_1^n(0)\,. \tag{11b}$$

The final wave function of the atom is given by

$$\psi(t) = a_1^l(1)\exp(-i\Omega_l t)|l\rangle + a_1^m(1)\exp(-i\Omega_m t)|m\rangle + a_1^n(0)\exp(-i\Omega_n t)|n\rangle\,. \tag{12}$$

C. Observables and PSA's

The observables associated with an atom may be calculated in terms of its PSA's. We will deal with two observables—the relative phase of the radiation emitted by the atom on a particular transition and the probability of finding the atom in a particular energy state. If an atom's wave function has the form

$$\psi(t) = A^s\exp(-i\Omega_s t)|s\rangle + A^{s'}\exp(-i\Omega_{s'} t)|s'\rangle\,, \tag{13}$$

it follows that

$$\mathcal{E}_r \propto \langle s|O|s'\rangle A^{s'}(A^s)^*\exp[-i(\Omega_{s'} - \Omega_s)t] + \text{c.c.}\,, \tag{14}$$

where $\mathcal{E}_r$ is the electric field radiated by the atom on the $|s\rangle$-$|s'\rangle$ transition and O is an operator corresponding to the multipole moment responsible for the radiation. Expanding A^s and $A^{s'}$ according to Eq. (3), we have

$$\mathcal{E}_r \propto \langle s|O|s'\rangle \sum_{i,i'} a_{i'}^{s'}(n_r')[a_i^s(n_r)]^* \times \exp[-i(\Omega_{s'} - \Omega_s)t] + \text{c.c.} \tag{15}$$

The net electric field emitted by the atom can be thought of as being the sum of a number of *components each of which in general has a different phase*. At certain times after excitation the relative phase of particular *components* of the electric field may be ordered throughout the sample in various ways (to be discussed below).

The wave function of Eq. (13) indicates that the probability of finding the atom in state $|s\rangle$, ρ_{ss}, obeys

$$\rho_{ss} \propto A^s (A^s)^* \propto \sum_{i,i'} a_i^s(n_\tau)[a_{i'}^s(n_\tau')]^* . \tag{16}$$

As in the case of the emitted electric field, the population density in state $|s\rangle$ can be thought of as consisting of a number of components each of which corresponds to a different product of PSA's. The population density corresponding to some components may be ordered throughout the sample at certain times after the excitation sequence.

III. TRAVELING-WAVE EXCITATION

A. Single atom

We now specialize to traveling-wave excitation pulses. Let the jth pulse have area θ_j, wave vector $\vec{k}_j$, and correspond to exact resonance with the transition between two arbitrary states denoted by $|s\rangle$ and $|s'\rangle$. The electric field of excitation pulse j then has the form

$$\mathcal{E}_j(t)\exp[-i(|\Omega_s - \Omega_{s'}|t - \vec{k}_j\cdot\vec{r})] + \text{c.c.} \tag{17}$$

We assume that the pulse is sufficiently short to allow the neglect of atomic motion throughout its duration. We consider a particular atom whose initial wave function is given by Eq. 4, and denote its position at the time t_j as $\vec{r}_j$.

As discussed in the previous section the effect of an excitation pulse on a general PSA $a_i^s(n_\tau)$ is summarized by the transformation equation

$$a_i^s(n_\tau) \rightarrow a_i^s(n_\tau+1), a_{i'}^{s'}(n_\tau) . \tag{18}$$

A straightforward application of the formalism developed in Ref. 27 relates the new PSA's to the old PSA's as follows:

$$a_i^s(n_\tau+1) = \cos(\theta_j/2) a_i^s(n_\tau) , \tag{19a}$$

$$a_{i'}^{s'}(n_\tau) = i\sin(\theta_j/2)\exp(i\epsilon_j \vec{k}_j\cdot\vec{r}_j) a_i^s(n_\tau) , \tag{19b}$$

where

$$\epsilon_j = +1(-1) \text{ if } \Omega_{s'} > \Omega_s (\Omega_{s'} < \Omega_s) .$$

These equations can be used to relate any PSA generated by a series of excitation pulses to the initial PSA $a_1^1(0)$.

Consider a particular PSA $a_q^p(N_\tau)$ which is associated with the state $|p\rangle$ and is assumed to have been generated through the action of a sequence of laser pulses on an atom initially described by the wave function of Eq. (4). As indicated within the parentheses, there were N_τ excitation pulses which modified the PSA's amplitude without changing the state to which it was associated. If there were N_t excitation pulses which did change the state to which the PSA was associated, then repeated application of Eq. (19) yields

$$a_q^p(N_\tau) = a_1^1(0)\left(\prod_{j=1}^{N_\tau}\cos(\theta_j/2)\right)\left(\prod_{j=1}^{N_t} i\sin(\theta_j/2)\exp[i\epsilon_j\vec{k}_j\cdot\vec{r}_j]\right), \tag{20}$$

The index j runs over those excitation pulses relevant to the evolution of $a_q^p(N_\tau)$. This will be made clearer in the next sections.

B. Sample as a whole

In the preceding sections, we have discussed the response of a particular atom to a series of laser-excitation pulses. Our ultimate objective, however, is to determine if and when the sample as a whole displays *order*. Here *order* is defined as a nonthermal variation of an observable (such as polarization, population density, etc.) with position (velocity) after averaging over atoms with all velocities at each position (with all positions for each velocity). To determine when ordering takes place, we must find an expression for the PSA's of atoms as a function of position $\vec{r}$ and velocity $\vec{v}$.

Fortunately, the assumption of time-independent $\vec{v}$ allows us to express the excitation positions of atoms at $\vec{r}$ at time t according to

$$\vec{r}_j = \vec{r} - \vec{v}(t - t_j) , \tag{21}$$

where $\vec{v}$ is the atom's velocity. Substituting Eq. (21) into Eq. (20), we obtain

$$a_q^p(N_\tau) = a_1^1(0) f_q^p e^{i\vec{R}_q^p\cdot\vec{r}} e^{-i\vec{v}_q^p\cdot\vec{v}} , \tag{22}$$

where

$$f_q^p \equiv \left(\prod_{j=1}^{N_\tau}\cos(\theta_j/2)\right)\left(\prod_{j=1}^{N_t} i\sin(\theta_j/2)\right) , \tag{23a}$$

$$\vec{K}_q^p \equiv \sum_{j=1}^{N_t} \epsilon_j \vec{k}_j , \tag{23b}$$

and

$$\vec{\varphi}_q^p = \sum_{j=1}^{N_t} \epsilon_j \vec{k}_j (t - t_j) = \vec{K}_q^p t - \sum_{j=1}^{N_t} \epsilon_j \vec{k}_j t_j . \tag{23c}$$

Equation (22) provides the form of the post-excitation PSA's of atoms throughout the sample as a function of their instantaneous position and velocity. As we will see the quantity $\vec{\varphi}_q^p$ is of special significance and is denoted the *velocity-dependent phase* (VDP) *coefficient*.

From Eqs. (15) and (16) we see that the calculation of observable properties of an atom often involves scalar products of PSA's of the form $a_q^p(N_\tau)[a_{q'}^{p'}(N_\tau')]^*$. Using Eq. (22), we have

$$a_q^p(N_\tau)[a_{q'}^{p'}(N_\tau')]^* = f_q^p (f_{q'}^{p'})^* \exp(i\vec{K}_x \cdot \vec{r}) \exp(-i\vec{\varphi}_x \cdot \vec{v}) , \tag{24}$$

where we assume that $a_1^1(0)$ in Eq. (22) is common to both PSA's and $a_1^1(0) = 1$. We define here $\vec{K}_x \equiv \vec{K}_q^p - \vec{K}_{q'}^{p'}$ and $\vec{\varphi}_x \equiv \vec{\varphi}_q^p - \vec{\varphi}_{q'}^{p'}$, respectively, as the wave vector and VDP coefficient associated with the observable x.

IV. BASIC DIAGRAMS

A. Definitions and examples

As we now demonstrate, the characteristics of the wave function which are important in the study of reordering processes in general and optical echoes in particular can be displayed in a simple diagrammatic form. *A diagram consists of a plot of the velocity-dependent phase coefficient of each* PSA *as a function of time*. One axis of the diagram is reserved for the time. The other axes are used to represent the components of $\vec{\varphi}(t)$ for each PSA along various spatial directions. Examining the form of $\vec{\varphi}(t)$ for an arbitrary PSA [see Eq. (23c)], we see that if all the laser pulses propagate with either sense along a particular direction, say $\hat{z}$, $\vec{\varphi}(t)$ is always parallel to $\pm\hat{z}$, and the diagrams may be restricted to two dimensions. Similarly, excitation pulses which are confined to a plane may be represented in a three-dimensional diagram. For the sake of simplicity, we restrict our attention in the following examples to collinear excitation pulses and two-dimensional diagrams. If we assume that the laser pulses propagate along $\pm\hat{z}$, our diagrams consist of a plot of $\vec{\varphi}(t) \cdot \hat{z} = \varphi_z(t)$ versus time.

Consider a sample in which all atoms initially reside in a state $|l\rangle$ [see Fig. 1(a) and Eq. (4)]. Since in an unprepared sample the atoms are not expected to show any special ordering with velocity, the VDP coefficient of the single existing PSA may be set equal to zero. Figure 2(a) gives the appropriate diagram. The single line indicates that there is only one PSA. Its lack of a time-dependent VDP coefficient is indicated by the fact that the line is horizontal. *The character of the line* (i.e., *solid) specifies with which energy state the* PSA *is associated.* We choose a solid line to represent the state $|l\rangle$.

We study the diagrams which result after each of a series of three laser pulses (designated by the subscripts 1, 2, and 3, where $t_1 < t_2 < t_3$) all of which are resonant with the $|l\rangle$-$|m\rangle$ transition. We assume $\Omega_m > \Omega_l$. Figure 2(b) shows a diagram which represents the action of pulse 1 (here $\vec{k}_1 \| \hat{z}$). At $t = t_1$, the initial PSA (solid line $t < t_1$) is transformed according to Eq. (5) into two PSA's. The VDP coefficient of the PSA which remains in $|l\rangle$ is unaffected; hence, the solid line continues unaltered for $t > t_1$. The PSA transferred to state $|m\rangle$, (state $|m\rangle$ is represented by a dashed line) acquires a VDP coefficient of $\epsilon_1 \vec{k}_1 (t - t_1)$ $= k_1 (t - t_1)\hat{z}$. Because the z component of this PSA's VDP coefficient increases with time, the dashed line representing the transferred PSA branches off from the original solid line with positive slope. Note that the amplitude associated with each PSA is not indicated in the diagram, but can easily be ascertained using Eq. (22). If we instead specify that $\Omega_m < \Omega_l$ or $\vec{k}_1 \| -\hat{z}$ (but not both), the dashed line in Fig. 2(b) will branch off toward the bottom of the page.

After the action of the second pulse, which has $\vec{k}_1 = \vec{k}_2$, we obtain the diagram shown in Fig. 2(c) [see also Fig. 1(c)]. As usual the VDP-coefficient lines representing the PSA's not transferred by the second pulse continue unaltered through $t = t_2$. The VDP coefficient of the PSA's transferred out of their initial state is modified; consequently, the new VDP-coefficient lines representing them branch away at $t = t_2$ from the original VDP-coefficient lines. The new solid (dashed) line represents the PSA transferred from $|m\rangle \rightarrow |l\rangle$ ($|l\rangle \rightarrow |m\rangle$). The z-component VDP coefficient of the PSA's transferred from $|l\rangle$-$|m\rangle$ at both $t = t_1$ and $t = t_2$ increases at the same rate; consequently, the dashed lines originating at $t = t_1$ and $t = t_2$ are parallel. From Eq. (23c), the new solid line has the VDP coefficient

$$\epsilon_1 \vec{k}_1 (t - t_1) + \epsilon_2 \vec{k}_2 (t - t_2) = k_1 (t_2 - t_1)\hat{z} ,$$

where we have used $\epsilon_1 = 1$, $\epsilon_2 = -1$, and $\vec{k}_1 = \vec{k}_2 \| \hat{z}$. If the second pulse is counterpropagating with respect to the first, we obtain a quite different diagram which is shown in Fig. 2(d).

Finally, a diagram which includes the effect of a third laser pulse, whose wave vector $\vec{k}_3$ satisfies $\vec{k}_1 = \vec{k}_2 = -\vec{k}_3$, is shown in Fig. 2(e). As usual,

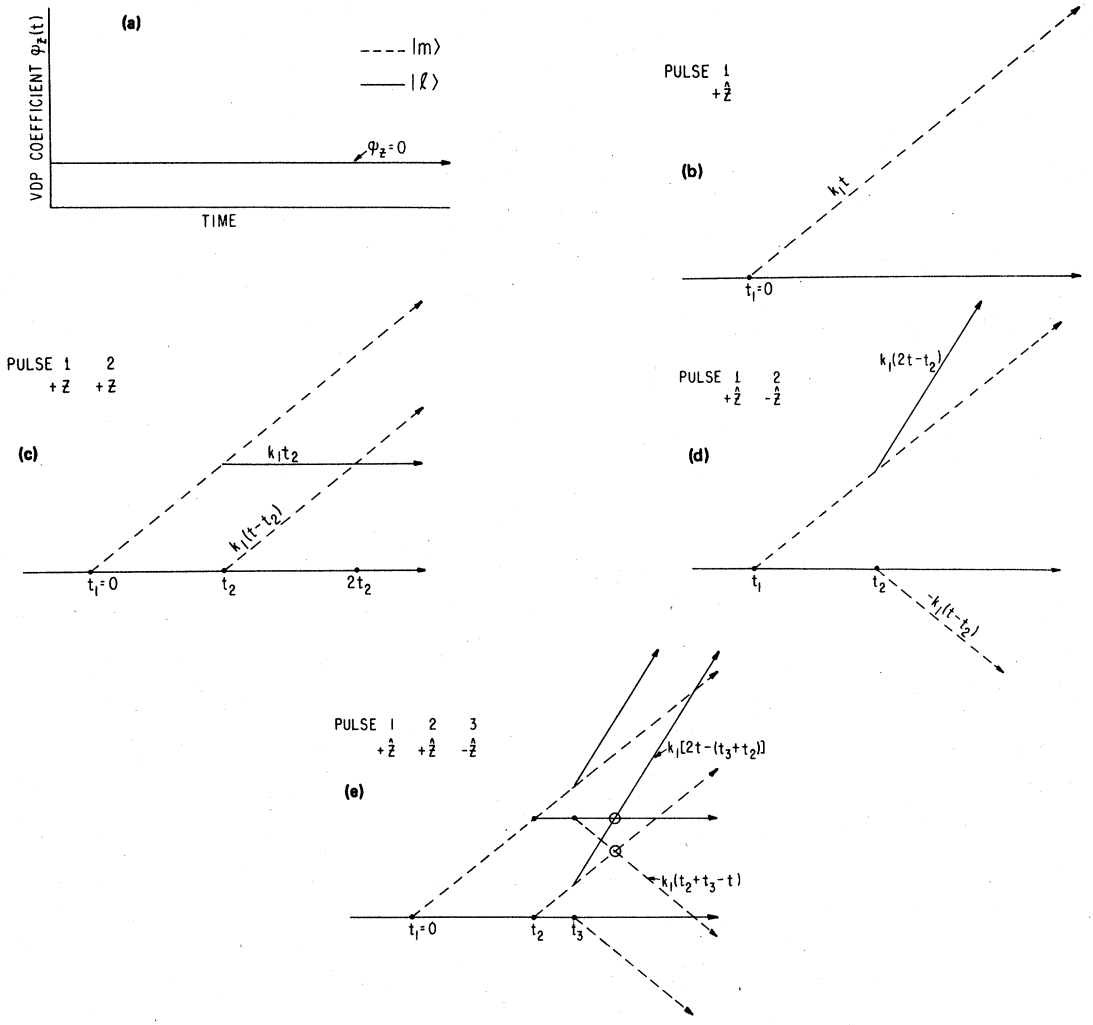

FIG. 2. (a) A diagram which displays the time evolution of the velocity-dependent-phase (VDP) coefficient of a single PSA in the absence of laser excitation. The vertical axis is the z component of the VDP coefficient and the horizontal axis is the time. The fact that the VDP-coefficient trajectory is represented by a solid line indicates that the associated PSA corresponds to state $|l\rangle$. (b) A VDP-coefficient diagram representing the macroscopic properties of a sample after the occurence of a single-laser excitation pulse at the time $t_1=0$. The axes shown in Fig. 2(a) are omitted in subsequent figures for simplicity. The dashed VDP-coefficient trajectory represents the PSA transferred by the pulse from state $|l\rangle$ to $|m\rangle$. As indicated in the figure the laser pulse is assumed to propagate along $+\hat{z}$. (c) The VDP coefficient diagram representing the action of two copropagating laser pulses. The intersection of a dashed and solid line at $t=2t_2$ indicates the occurrence of the well-known two-pulse photon echo. The VDP coefficient of each of the two PSA's transferred by the second pulse is shown next to the line representing it. (d) The VDP-coefficient diagram representing a sequence of two counter-propagating pulses. Note that there is no longer an intersection of lines at $t=2t_2$ indicating that the two-pulse photon echo cannot occur with counter-propagating excitation pulses. (e) The VDP-coefficient diagram representing the action of two copropagating laser pulses followed by a third counter-propagating pulse. If, as shown, the third pulse occurs before $t=2t_2$, similar lines intersect and indicate the formation of grating echoes.

new VDP-coefficient lines, representing transferred PSA's, branch off from the existing VDP-coefficient lines at $t=t_3$. The VDP coefficient of each transferred PSA is simply modified by the addition of a term $\epsilon_3\vec{k}_3(t-t_3)=-\epsilon_3 k_3(t-t_3)\hat{z}$.

B. General rules for construction of diagrams

We can write a few simple rules which allow the construction of two-dimensional diagrams appropriate to an arbitrary sequence of traveling-wave

excitation pulses which propagate along $\pm\hat{z}$.

(1) A diagram generally starts with a single VDP-coefficient line representing a PSA associated with a certain initial state, e.g., the ground state.

(2) A particular type of line (e.g., solid, dashed, etc.) is used to represent the VDP coefficient of all PSA's associated with a given state.

(3) If a traveling-wave laser pulse couples a state $|s\rangle$ to a state $|s'\rangle$ at the time t_j, all VDP-coefficient lines associated with state $|s\rangle$ will branch at $t=t_j$ into two parts. One part will continue unaltered as to slope and type. The other part will be of the line-type used to describe state $|s'\rangle$, and will have a factor $\epsilon_j \vec{k}_j \cdot \hat{z}$ added to its slope. As above $\epsilon_j = +1$ if $\Omega_{s'} > \Omega_s$ and -1 otherwise.

These rules are easily generalized to the case of coplanar excitation pulses.

V. INTERPRETATION OF THE DIAGRAMS

A. Intersections of dissimilar lines

The presence of dissimilar lines in a diagram implies that there exist PSA's which are associated with more than one energy eigenstate, or equivalently that the atoms are in a linear superposition of states. We consider two levels $|l\rangle$ and $|m\rangle$ which have PSA's associated with them. As in the preceding section, assume $\Omega_m > \Omega_l$. We denote the PSA in state $|l\rangle$ and $|m\rangle$ as a^l and a^m, respectively. (Since we restrict our attention to only these two PSA's the subscripts used above to specify PSA's have been omitted.)

Because the atoms are in a linear superposition of states, there will generally exist a polarization in the sample which oscillates at the $|l\rangle$-$|m\rangle$ transition frequency and corresponds to a particular radiation multipole operator O. The contribution $p^O_{lm}(\vec{r},\vec{v})$ of a particular atom which is located at the position $\vec{r}$ and has the velocity $\vec{v}$ to the net polarization is given by

$$\begin{aligned} p^O_{lm}(\vec{r},\vec{v}) &= \langle l|O|m\rangle\, a^m(a^l)^* \exp[-i(\Omega_m-\Omega_l)t] + \text{c.c.} \\ &= \langle l|O|m\rangle\, f^m(f^l)^* e^{i\vec{K}_{\text{pol}}\cdot\vec{r}} \\ &\quad \times e^{-i\vec{\varphi}_x(t)\cdot\vec{v}} e^{-i(\Omega_m-\Omega_l)t} + \text{c.c.}\,. \end{aligned} \tag{25}$$

Here Eq. (24) has been employed to obtain the general form of $a^m(a^l)^*$. The net polarization at $\vec{r}$, $P^O_{lm}(\vec{r})$, is obtained by integrating $p^O_{lm}(\vec{r},\vec{v})$ over the velocity distribution $f(\vec{v})$, i.e.,

$$\begin{aligned} P^O_{lm}(\vec{r}) &= \langle l|O|m\rangle f^m(f^l)^* e^{i\vec{K}_{\text{pol}}\cdot\vec{r}} F(\vec{\varphi}_{\text{pol}}) e^{-i(\Omega_m-\Omega_l)t} \\ &\quad + \text{c.c.}, \end{aligned} \tag{26}$$

where

$$F(\vec{\varphi}_{\text{pol}}) = \int d\vec{v} f(\vec{v}) \exp(-i\vec{\varphi}_{\text{pol}}(t)\cdot\vec{v})\,. \tag{27}$$

It is immediately clear that $|P^O_{lm}(\vec{r})|$ is large only when $|\vec{\varphi}_{\text{pol}}| \cong 0$. This occurs precisely when dissimilar VDP coefficient lines representing the PSA's a^l and a^m intersect.

In Fig. 2(b) the dashed and solid lines branch from a common point at $t=t_1$. The initial closeness of the lines (and in fact their intersection at $t=t_1$) indicates that immediately after excitation the sample has a net polarization. The magnitude of this polarization decreases as the lines diverge. In Fig. 2(c), a solid and dashed line intersect at $t=t_1+2t_2$. The corresponding net polarization gives rise to the two-pulse photon echo.

In a sample large compared to $\lambda_e = 2\pi c/|\Omega_m-\Omega_l|$, the intersection of dissimilar VDP-coefficient lines and the concomitant appearance of a net polarization (assuming of course that $\langle l|O|m\rangle \neq 0$) does not guarantee the emission of coherent radiation by the sample. The electric field emitted from the net polarization of Eq. (26) located at $\vec{r}$ has the form

$$\mathcal{E}_e(\vec{r},\vec{R}) \propto \frac{F(\vec{\varphi}_{\text{pol}})P^O(\hat{n})}{|\vec{R}-\vec{r}|} \exp[i(\vec{K}_{\text{pol}}\cdot\vec{r})] \exp\{-i[\Omega_{ml}t - \vec{k}_e\cdot(\vec{R}-\vec{r})]\} + \text{c.c.}, \tag{28}$$

where $\vec{R}$ is a distant point of observation, $\hat{n} \equiv (\vec{R}-\vec{r})/|\vec{R}-\vec{r}|$, $\vec{k}_e \equiv \Omega_{ml}\hat{n}/c$, $\Omega_{ml} \equiv \Omega_m - \Omega_l$, and $P^O(\hat{n})$ represents the angular distribution of radiation from the Oth multipole moment. The total electric field at $\vec{R}$ is obtained by integrating Eq. 28 over $\vec{r}$ throughout the sample volume:

$$\mathcal{E}_e(\vec{R}) \propto \frac{F(\vec{\varphi}_{\text{pol}})P^O(\hat{n})}{|\vec{R}|} \exp[-i(\Omega_{ml}t - \vec{k}_e\cdot\vec{R})] \int_{\text{sample}} d\vec{r} \exp[-i(\vec{k}_e - \vec{K}_{\text{pol}})\cdot\vec{r}]. \tag{29}$$

We assume in Eq. (29), that $\vec{R}$ is sufficiently far from the sample that it is possible to treat $\vec{k}_e$, $|\vec{R}-\vec{r}| \cong |\vec{R}|$, and $P^O(\hat{n})$ as constants during the integration over $\vec{r}$. The integral over $\vec{r}$ can only be large if $|\vec{k}_e| \cong |\vec{K}_{\text{pol}}|$. If this condition is satisfied, the sample is said to be *phase-matched*, and coherent emission may occur in directions $\vec{k}_e \cong \vec{K}_{\text{pol}}$.

The quantity $\vec{K}_{\text{pol}} \equiv \vec{K}^m - \vec{K}^l$ can be obtained rather quickly using (Eq. 23b) to obtain $\vec{K}^m$ and $\vec{K}^l$ for the PSA's involved. The wave vectors associated

with the $t = t_1 + 2t_2$ intersection of solid and dashed lines in Fig. 2(c) are as follows: $\vec{K}^m = \vec{k}_1$, $\vec{K}^l = 0$, and $\vec{K}_{pol} = \vec{k}_1$. Here $\vec{K}^m$ corresponds to the dashed line. Since $|\vec{k}_1| = \Omega_{ml}/c$, the photon echo is phase-matched (provided as was assumed that the two excitation pulses copropagate). The wave vector of the polarization can also be obtained directly from the diagram, as it can be deduced from the difference in slope of the intersecting lines.

B. Parallel lines of the same character

Consider a diagram in which there are two parallel VDP-coefficient lines both of which correspond to the energy eigenstate $|l\rangle$ [see Fig. 2(c)]. The lines correspond to two l-state PSA's which we denote by a_1^l and a_2^l. Neglecting any other PSA's associated with $|l\rangle$, the expectation value of finding an atom in state $|l\rangle$, ρ_{ll}, is given by

$$\rho_{ll} = (a_1^l + a_2^l)(a_1^l + a_2^l)^* = |a_1^l|^2 + |a_2^l|^2 + 2\,\mathrm{Re}[a_1^l (a_2^l)^*], \tag{30}$$

which can be rewritten as

$$\rho_{ll} = \alpha + \beta \cos^2(\chi_{12}(\vec{r}, \vec{v}, t)/2), \tag{31}$$

where χ_{12} represents the phase of $a_1^l (a_2^l)^*$ and α and β are constants. The fact that the VDP-coefficient lines of the two PSA's are parallel implies that $\vec{K}_x$ of Eq. (24) equals zero. Consequently [see Eq. (24)], the phase χ_{12} for parallel lines, denoted by χ_{12}^p, is independent of time and position, but it is generally not independent of velocity. Using Eq. (22) for a_1^l and a_2^l, Eq. (24) for $a_1^l (a_2^l)^*$, and with $\vec{K}_1^l = \vec{K}_2^l$, we have

$$\chi_{12}^p(\vec{v}) = \sum_{j_1=1}^{N_{t_1}} \epsilon_{j_1} \vec{k}_{j_1} \cdot \vec{v} t_{j_1} - \sum_{j_2=1}^{N_{t_2}} \epsilon_{j_2} \vec{k}_{j_2} \cdot \vec{v} t_{j_2} + (N_{t_1} - N_{t_2})\pi/2. \tag{32}$$

Substituting Eq. (32) for χ_{12}^p into the expression for ρ_{ll} it can be seen that the number density of atoms in state $|l\rangle$ is modulated as a function of $\vec{v}$.

We see in Fig. 2(c) that two copropagating laser-excitation pulses produce both parallel solid and parallel dashed lines. Evaluating Eq. (31) under the diagram conditions we find that

$$\chi_{12}^p = (k_2 t_2 - k_1 t_1) v_z - \pi = k_1 (t_2 - t_1) v_z - \pi.$$

The population is modulated with v_z with a period $2\pi/k_1(t_2 - t_1)$. This modulation is independent of time and position. Note that the *sum* of the population in states $|l\rangle$ and $|m\rangle$ displays no modulation in v_z space.

A third laser pulse, whose action is represented diagrammatically in Fig. 2(e), can transform the ordering of *population versus* v_z into an ordering of *polarization versus position*. Consider the two parallel solid lines which exist in the figure for $t > t_2$. At the time t_3, the third pulse causes a dashed line to branch downward away from each solid line. The upper of these dashed lines intersects the lower solid line a time $(t_2 - t_1)$ after t_3. The echo which results is generally known as the stimulated photon echo.[12,14] Note that between t_2 and t_3, all the VDP-coefficient lines except the two solid ones could be eliminated and the stimulated echo would still occur. The same discussion applies to the two parallel dashed lines that exist between t_2 and t_3. The stimulated echo may be independently produced from velocity ordering of population in either the $|l\rangle$ or $|m\rangle$ states.

C. Intersection of similar lines

As in the preceding section, the two similar lines referring, say to state $|l\rangle$, lead to an expression for ρ_{ll} given by Eq. (31). The fact that the lines cross, however, leads to a different expression for χ_{12}. We use χ_{12}^c to denote the phase of $a_1^l (a_2^l)^*$ at the time the two similar VDP lines cross. Since the lines cross, we know that $\vec{\varphi}_1^l$ and $\vec{\varphi}_2^l$ in the expressions [see Eq. (22)] for a_1^l and a_2^l must be equal. Consequently, χ_{12}^c is dependent only on $\vec{r}$ and has the form

$$\chi_{12}^c(\vec{r}) = (\vec{K}_1^l - \vec{K}_2^l) \cdot \vec{r} + (N_{t_1} - N_{t_2})\pi/2. \tag{33}$$

The atomic number density in state $|l\rangle$ then has the form

$$\rho_{ll} = \alpha + \beta \cos^2\{[(\vec{K}_1^l - \vec{K}_2^l) \cdot \vec{r} + (N_{t_1} - N_{t_2})\pi/2]/2\}. \tag{34}$$

This expression for ρ_{ll} shows that for the particular time that the similar lines cross, the overall density of atoms in state $|l\rangle$ varies periodically with position. The atoms in state $|l\rangle$ momentarily form a spatial grating (a grating echo) which can be detected by scattering a laser from it.[13]

In Fig. 2(e), a sequence of two copropagating pulses followed by one counterpropagating pulse gives rise to a grating echo in both state $|l\rangle$ and $|m\rangle$. From Eq. (34) it is clear that these gratings are characterized by the wave vector $2\vec{k}_1$.

D. Parallel lines of dissimilar character

Using the same nomenclature as in Sec. V A, we see that the presence of parallel dissimilar lines in a diagram implies that $\vec{K}_{pol}$ of Eq. (26) vanishes. Thus the phase of the polarization P_{lm}^o (which corresponds to the two PSA's represented by the paralled dissimilar lines) *is independent* of *position* but unless $\vec{\varphi}_{pol} = 0$ *is modulated in velocity space*. Among other things, the

position indepence of P^o_{lm} can give rise to interesting grating echo effects. Parallel dissimilar lines can quite generally be created by appropriate coplanar excitation pulses.

VI. TRILEVEL ECHOES

Laser pulses, which successively excite coupled transitions, can lead to a wide range of interesting and useful echo effects.[7,30,31] One such effect, which has been termed the sum-frequency trilevel echo (SF echo) is described here diagrammatically. The SF echo was chosen because of its proven utility in measuring the collisional broadening rates of two-photon transitions between ground and Rydberg excited states of the same parity.[30]

The three energy levels involved are depicted in Fig. 3a. We assume that $\Omega_{nm} > \Omega_{ml}$. The relative times, frequencies, and propagation directions of the three requisite pulses are shown in Fig. 3(b). The SF echo [shown as the dashed pulse in Fig. 3(b)] occurs at the time $t_e > t_3$ on the $|l\rangle - |m\rangle$ transition. The line-types used in the diagram to represent the three energy states are defined in Fig. 3(a).

The diagram, which is constructed according to the rules of Sec. IV B, is shown in Fig. 3(c). Three intersections between dissimilar lines are shown in the figure. The intersection marked "A" indicates a rephasing on the electric-dipole forbidden $|l\rangle - |n\rangle$ transition. Intersection "C" corresponds to the two-pulse photon echo produced by the two pulses resonant with the $|m\rangle - |n\rangle$ transition. The SF echo is indicated by intersection "B". Note that if $\Omega_{nm} < \Omega_{ml}$, the dot-dash line originating at t_2 would have a positive slope and the SF echo would not occur. Similarly, if pulse 3 occurred before intersection "A" the SF echo would not occur. The SF echo can be thought of as a third-pulse induced rephasing of "A".

Since the VDP coefficient of the solid line can be taken as zero, we can obtain the SF echo time by simply solving for the time which makes the VDP coefficient of the intersecting dashed line equal to zero as well. We have

$$k_{ml}(t_e - t_1) - k_{nm}(t_e - t_2) + k_{nm}(t_e - t_3) = 0\,, \tag{35}$$

or

$$t_e = t_1 + \frac{k_{nm}}{k_{ml}}(t_3 - t_2)\,. \tag{36}$$

Here $k_{ij} \equiv \Omega_{ij}/c$.

From Eqs. (22), (24), and (29), the wave vector of the echo $\vec{k}_e$ is equal to the wave vector of the first pulse, i.e., $\vec{k}_e = k_{ml}\hat{z}$.

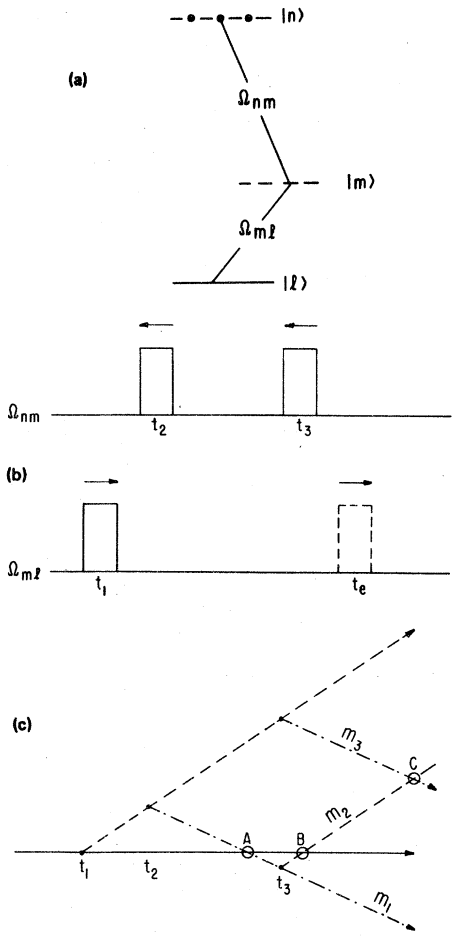

FIG. 3. The relative energies of the three energy levels involved in the sum-frequency trilevel echo. The line-type used to designate each level is indicated in this figure. (b) The frequencies, times, and relative propagation directions (indicated by the arrows) of the three sum-frequency trilevel echo excitation pulses. The dashed pulse represents the echo. (c) The VDP-coefficient diagram representing the action of the three pulses described in Fig. 3(b). Intersection "B" represents the occurrence of the sum-frequency trilevel echo. The slopes m_j $(j=1,2,3)$ shown are given by: $m_1 = (k_1 - k_2)t + (k_2 t_2 - k_1 t_1)$, $m_2 = k_1 t - (k_1 t_1 - k_2 t_2 + k_3 t_3)$, and $m_3 = (k_1 - k_3)t + (k_3 t_3 - k_1 t_1)$, where k_j is the magnitude of the jth pulses's wave vector.

VII. STANDING-WAVE EXCITATION

In Fig. 2(b) we presented a diagram representing the action of a single traveling-wave excitation pulse. A dramatically different but analogous diagram for a single standing-wave (SW) excitation pulse is given in Fig. 4.

As in Fig. 2(b) the solid and dashed lines represent PSA's associated with the initial, $|l\rangle$, and final, $|m\rangle$, state, respectively. The SW pulse is

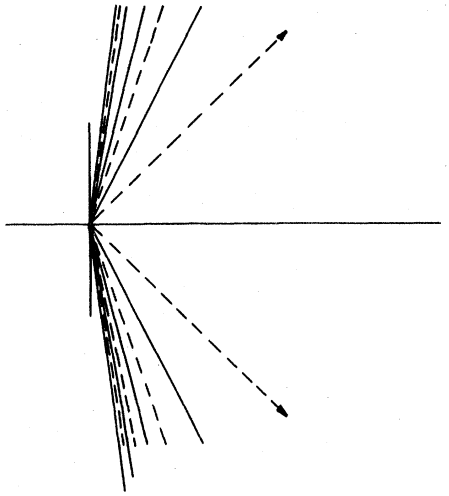

FIG. 4. The VDP coefficient diagram which represents the action of a single standing-wave pulse on a PSA. The solid line refers to the initial state with which the PSA is associated and the dashed line to the state coupled to by the standing-wave field.

assumed to have the form $\mathcal{E}(t)\cos(|\Omega_m - \Omega_l|t)\cos(\vec{k}_j\cdot\vec{r})$. A traveling-wave pulse has a constant area θ_j and a position-dependent phase. On the other hand, a SW pulse has a constant phase and a position-dependent area. For the SW we have $\theta_j(\vec{r}) = \theta_j^0\cos(\vec{k}_j\cdot\vec{r})$.

The SW-transformation equation analogous to Eq. (19) is given by

$$a_i^l(n_r+1) = \cos[\theta_j(\vec{r}_j)/2]\,a_i^l(n_r),$$
$$a_{i'}^m(n_r) = i\sin[\theta_j(\vec{r}_j)/2]\,a_i^l(n_r). \tag{37}$$

We can use Bessel functions of the first kind to expand the coefficients in Eq. (37) according to

$$\cos[(\theta_j^0/2)\cos(\vec{k}_j\cdot\vec{r}_j)] = \sum_{n=-\infty}^{\infty}(-1)^n e^{2in(\vec{k}_j\cdot\vec{r}_j)}J_{2n}(\theta_i^0/2), \tag{38a}$$

and

$$\sin[(\theta_j^0/2)\cos(\vec{k}_j\cdot\vec{r}_j)] = \sum_{n=-\infty}^{\infty}(-1)^n e^{i(2n+1)(\vec{k}_j\cdot\vec{r}_j)}J_{2n+1}(\theta_j^0/2). \tag{38b}$$

If Eq. (21) is used to eliminate $\vec{r}_j$ in Eq. (38), we see that the single initial PSA associated with state $|l\rangle$ is divided into an infinite number of PSA's each characterized by a distinctive VDP coefficient. After the SW pulse, there is a PSA associated with state $|l\rangle$ for every VDP coefficient given by

$$2n\vec{k}_j(t-t_j), \quad n = (\ldots,-1,0,1,\ldots).$$

The amplitude of each PSA is proportional to $J_{2n}(\theta_j^0/2)$. For any θ_j^0, $|J_{2n}(\theta_j^0/2)|$ eventually decreases rapidly for $|n|$ above a certain value. Associated with the final state $|m\rangle$, there are PSA's having each of the VDP coefficients

$$(2n+1)\vec{k}_j(t-t_j), \quad n = (\ldots,-1,0,1,\ldots)$$

where the amplitude of each PSA varies as $J_{2n+1}(\theta_j^0/2)$.

The dramatic difference between the action of a traveling-wave pulse and that of a SW pulse has an intuitive interpretation. A traveling-wave pulse is characterized by a single wave vector, say $k_j\hat{z}$. Consequently, in a second-order interaction, where a PSA is transferred by the single pulse from $|l\rangle - |m\rangle - |l\rangle$, the VDP coefficient of the PSA is unchanged by the pulse. The same second-order interaction induced by a SW pulse may proceed via the $+k_j\hat{z}$ SW component from $|l\rangle - |m\rangle$ and the $-k_j\hat{z}$ component from $|m\rangle - |l\rangle$. The z-component VDP coefficient of the PSA is then modified by $2k_j(t-t_j)$. Generalizing, in the traveling-wave case all even-order interactions result in the PSA returning to state $|l\rangle$ and cause no modification of VDP. All odd-order interactions leave the PSA associated with state $|m\rangle$ and modify the z-component VDP coefficient of the PSA by $k_j(t-t_j)$. The net effect of a traveling-wave pulse then is only to create two PSA's distinguishable on the basis of VDP. In the SW case the $2n$th-order interaction ($n = 1, 2, \ldots$) which returns the PSA to $|l\rangle$ may, because of the interaction with the oppositely directed SW components, have a VDP coefficient as large as $2nk_j(t-t_j)$. Similarly, odd-order interactions which leave the PSA associated with state $|m\rangle$ may result in a VDP coefficient as large as $(2n+1)k_j(t-t_j)$.

The action of a SW pulse is represented diagrammatically according to the following rule: If a SW-laser pulse couples a state $|s\rangle$ to a state $|s'\rangle$ at the time t_j, all VDP-coefficient lines associated with state $|s\rangle$ will branch at the time t_j into two fans of lines. One fan, of the same type line associated with state $|s\rangle$, will have VDP lines different in slope from the original line by all *even* integral multiples of k_j. The other fan, of the line-type associated with state $|s'\rangle$, will have lines different in slope from the original line by all *odd* integral multiples of k_j.

VIII. CONCLUSION

We have outlined a broadly applicable diagrammatic technique for the analysis of laser-induced (re)ordering processes which is applicable to both gases and solids. The diagrams explain many echo phenomena in a clear and unified fashion which should lead to a deeper understanding of the

phenomena. It is to be expected that this diagrammatic approach will also facilitate the full utilization of (re)ordering effects in studies of both relaxation[6,9,12,14,20,30-34] and spectroscopy.[5,8,20] In many cases a reordering effect (e.g., an echo) can be designed using diagrams to yield the particular information desired.

ACKNOWLEDGMENT

This work was supported by the U. S. Joint Services Electronics Program (Contract No. DAAG29-79-C-0079) and by the U. S. Office of Naval Research (Contract No. N00014-78-C-517).

[1]For a review of work through 1978, see R. L. Shoemaker, Ann. Rev. Phys. Chem. 30, 239 (1979).
[2]C. K. N. Patel and R. E. Slusher, Phys. Rev. Lett. 20, 1087 (1968).
[3]B. Bölger and J. C. Diels, Phys. Lett. 28A, 401 (1968).
[4]R. G. Brewer and R. L. Shoemaker, Phys. Rev. Lett. 27, 631 (1971).
[5]R. L. Shoemaker and F. A. Hopf, Phys. Rev. Lett. 33, 1527 (1974).
[6]T. Baer and I. D. Abella, Phys. Lett. 59A, 371 (1976); Opt. Lett. 3, 170 (1978).
[7]T. Mossberg, A. Flusberg, R. Kachru, and S. R. Hartmann, Phys. Rev. Lett. 39, 1523 (1977).
[8]V. P. Chebotayev, N. M. Dyuba, M. I. Skvortsov, and L. S. Vasilenko, Appl. Phys. 15, 319 (1978).
[9]A. Flusberg, T. Mossberg, and S. R. Hartmann, Opt. Commun. 24, 207 (1978).
[10]P. Hu and H. M. Gibbs, J. Opt. Soc. Am. 68, 1630 (1978).
[11]A. Flusberg, T. Mossberg, R. Kachru, and S. R. Hartmann, Phys. Rev. Lett. 41, 305 (1978).
[12]T. Mossberg, A. Flusberg, R. Kachru, and S. R. Hartmann, Phys. Rev. Lett. 42, 1665 (1979); R. Kachru, T. W. Mossberg, and S. R. Hartmann, Opt. Commun. 30, 57 (1979).
[13]T. W. Mossberg, R. Kachru, E. Whittaker, and S. R. Hartmann, Phys. Rev. Lett. 43, 851 (1979). Grating echoes have also been investigated by Y. Fukuda, K. Yamada, and T. Hashi (private communication).
[14]M. Fujita, H. Nakatsuka, H. Nakanishi, and M. Matsuoka, Phys. Rev. Lett. 42, 974 (1979).
[15]C. V. Heer and R. L. Sutherland, Phys. Rev. A 19, 2026 (1979).
[16]R. Kachru, T. W. Mossberg, E. Whittaker, and S. R. Hartmann, Opt. Commun. 31, 223 (1979).
[17]I. D. Abella, N. A. Kurnit, and S. R. Hartmann, Phys. Rev. 141, 391 (1966).
[18]V. V. Samartsev and R. G. Usmanov, Zh. Eksp. Teor. Fiz. 72, 1702 (1977) [Sov. Phys.–JETP 45, 892 (1977)].
[19]W. H. Hesselink and D. A. Wiersma, Chem. Phys. Lett. 56, 227 (1978).
[20]Y. C. Chen, K. Chiang, and S. R. Hartmann, Phys. Rev. B 21, 40 (1980); P. F. Liao, P. Hu, R. Leigh, and S. R. Hartmann, Phys. Rev. A 9, 332 (1974).
[21]M. Scully, M. J. Stephen, and D. C. Burnham, Phys. Rev. 171, 213 (1968).
[22]G. M. Ershov and U. K. Kopvillem, Zh. Eksp. Teor. Fiz. 63, 279 (1972) [Sov. Phys.–JETP 36, 147 (1973)].
[23]T. M. Makhviladze and L. A. Shelepin, Zh. Eksp. Teor. Fiz. 62, 2066 (1972) [Sov. Phys.–JETP 35, 1080 (1972)].
[24]M. Aihara and H. Inaba, J. Phys. A 6, 1709 (1973); 6, 1725 (1973); Opt. Commun. 8, 280 (1973).
[25]A. I. Siraziev and V. V. Samartsev, Opt. Spektrosk. 39, 730 (1975) [Opt. Spectrosc. (USSR) 39, 413 (1975)].
[26]N. Shiren, Appl. Phys. Lett. 33, 299 (1978).
[27]T. W. Mossberg, R. Kachru, S. R. Hartmann, and A. M. Flusberg, Phys. Rev. A 20, 1976 (1979).
[28]R. P. Feynman, F. L. Vernon, Jr., and R. W. Hellworth, J. Appl. Phys. 28, 49 (1957).
[29]D. Grischkowsky, M. M. T. Loy, and P. F. Liao, Phys. Rev. A 12, 2514 (1975).
[30]R. Kachru, T. W. Mossberg, and S. R. Hartmann, Phys. Rev. A 21, 1124 (1980).
[31]T. W. Mossberg, E. Whittaker, R. Kachru, and S. R. Hartmann, Phys. Rev. A 22, 1962 (1980).
[32]W. H. Hesselink and D. A. Wiersma, Chem. Phys. Lett. 50, 51 (1977); T. J. Aartsma and D. A. Wiersma, *ibid.* 54, 415 (1978).
[33]P. R. Berman, J. M. Levy, and R. G. Brewer, Phys. Rev. A 11, 1668 (1975).
[34]R. Kachru, T. W. Mossberg, and S. R. Hartmann, J. Phys. B 13, L363 (1980).